



## Structural and Optical Properties of BaTiO<sub>3</sub> Thin Film Deposited on Quartz Substrate by Sol Gel Technique

Ms. Vandana Kaushik<sup>a</sup>, Dr. Manoj Kumar<sup>a</sup> and Dr. Anuj Kumar<sup>b</sup>

- a. Department of Physics, School of Physical Sciences, Starex University, Gurugram, India.
- b. Department of Physics, JC Bose University of Science and Technology, Faridabad, India

---

### Abstract

In this report thin films of Barium Titanate BaTiO<sub>3</sub> (BTO) was coated on quartz substrate using dip coating technique. X-ray diffraction analysis revealed the formation of BTO thin film with a cubic structure with orientations along (200) plane. Average crystallite size of the film was estimated to be 32.021 nm with dislocation density of value  $8.04484 \times 10^{-4} \text{ nm}^{-2}$ . SEM micrograph images observed the dense thin film with the presence of crack and flakes on the surface. EDX analysis observed the high purity of BTO thin film. UV spectroscopy depicted the high transparency of the BTO film in UV region and estimated values of with energy band gap and Urbach energy are 3.77 eV and 0.34456 eV respectively. All the analysis declared the BTO thin films to be suitable for various electro-optic applications.

**Key Words:** BaTiO<sub>3</sub> (BTO), BTO thin films, sol gel technique, dip coating technique, quartz surface

---

### 1. Introduction

Barium Titanate (BTO) with structure like perovskite has been increasingly desired ceramics because of its amazing ferroelectricity, large electro-optic coefficient and outstanding dielectric features with diverse applications such as thermistors, multilayer capacitors and many other electric applications [1]. BTO behaves as a dielectric material in spectrum range from the near UV to the near IR with relatively high refractive index and low optical losses and to be a metal oxide BTO fulfills many practical necessities such as stability, physical sturdiness and optoelectronic features that are tunable. It has high transmittance in the visible region and have great potential for various electro-optic applications. Extensive research has been done on BTO in the form a single crystal or ceramic BTO, whereas its thin films also have applications in diverse areas [2-5]. Thin films of BTO hold piezoelectric features along with dielectric and optical characteristics. BTO thin film with perovskite structure, possess significant features to be used in many solid-state devices such as sensors, multi-layer capacitors, thermistors, non-volatile memory devices and actuators[6-11]

Various techniques for synthesis have been employed for the fabrication of BTO thin films for example sputtering, hydrothermal method, chemical vapor deposition technique, electro-chemical reduction method, molecular beam epitaxy and sol-gel techniques etc. [12-22]. The sol-gel based deposition techniques have indubitably advantages like better homogeneity of the

composition of crystal, easy to control stoichiometry, easy to use, efficient to coat substrates with large and complex area and less processing expenses in comparison to the many other techniques [23-33]. The sol gel techniques require precursors in liquid form for the deposition over the surface of the substrates by spray method or dip coating or spin-coating followed by appropriate thermal treatment to remove the traces of solvents. Other advantages of the sol-gel techniques are non-vacuum requirement, easy processing at low temperature, better chemical homogeneity and uniform coating of film on large substrates[34]. In addition to all above this technique involves comparatively less equipment [35].

This paper reported fabrication of BTO thin film using solution based dip coating technique on quartz surface. The main goal is to investigate the structural and optical characteristics of fabricated BTO thin films.

### **Experimental Procedure**

#### *Materials*

In this report we used barium acetate (AR Grade) and titanium IV isopropoxide (assay > 99 %) as precursors and glacial acetic acid (AR Grade) as solvents for the preparation of the solution. Ethylene Glycol (AR Grade) was used as stabilizing agent.

#### *Synthesis and Characterization*

At the first step barium acetate as barium precursor was dissolved in glacial acetic acid to prepare 0.15 M solution and stirred at 70<sup>0</sup> C for 30 minutes . The titanium IV isopropoxide as precursor of titanium was added to solution drop wise in equimolar ratio followed by addition of 0.5 ml of ethylene glycol with constant stirring. The resulting clear solution was stirred and refluxed at 70<sup>0</sup>C for 1hr. Then, this clear solution was hydrolyzed by adding 30 ml of deionized (DI) water and kept stirring at magnetic stirrer for 4 hrs. Before deposition of film the surface of quartz substrate was cleaned well with acetone, methanol and DI water. The precursor solution was coated on the clean surface of quartz substrate by dip coating method at 10cm/min speed and then dried on hot plate at 70<sup>0</sup> C to remove the solvents. The dip coating and preheating were repeated several times in order to get desired thickness of the precursor films. The final sample was annealed at temperature 650<sup>0</sup> C. The whole process has been demonstrated by fig. 1.

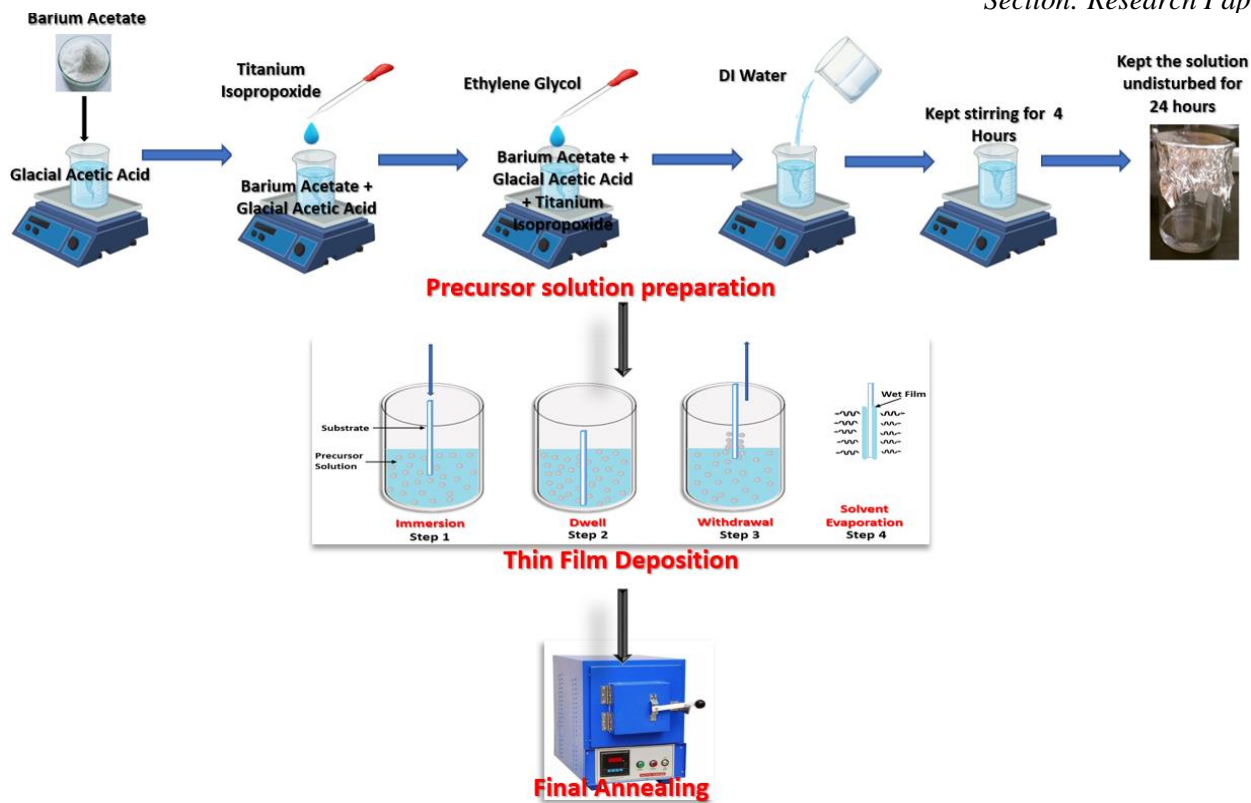


Fig. 1: Step by step process to fabricate the BTO thin film on quartz substrate

## 2. Results & Discussion

### 2.1. XRD Analysis

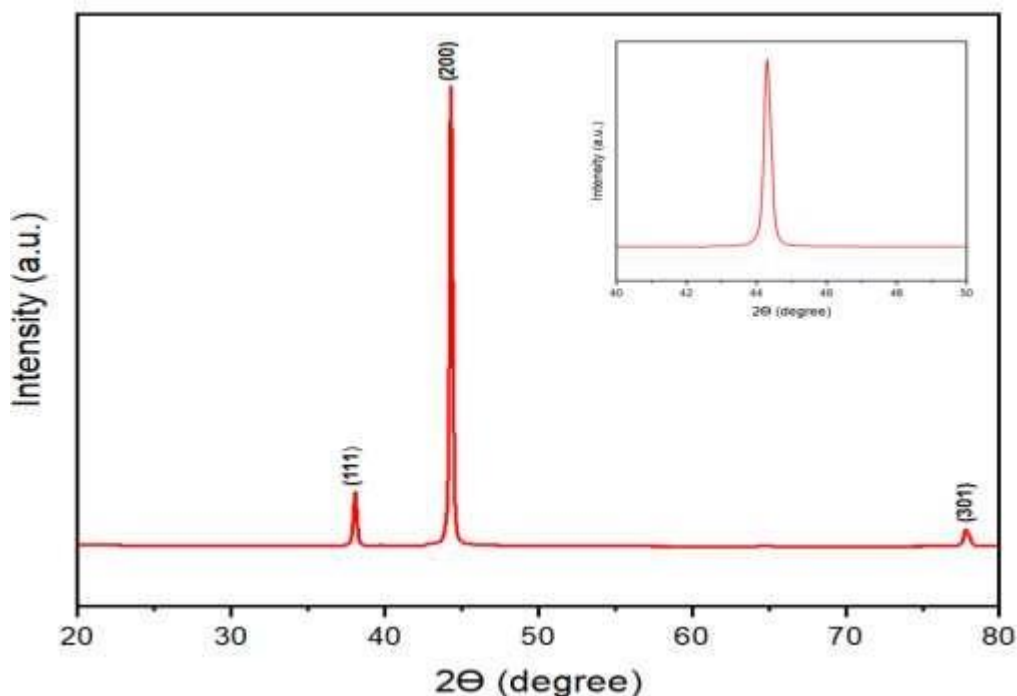


Fig. 2. XRD pattern of BTO thin films fabricated on quartz substrate.

The XRD pattern of BTO thin film deposited on quartz substrate is shown in fig. 2. The Bragg reflections from the (111), (200), and (301) planes are accounted for by the diffraction peaks at 38.08°, 44.3°, and 77.4° respectively. The absence of peaks from other phases indicates a high degree of purity for the BTO thin films. The intensity of (200) peak was found to be maximum and the lower 2θ value of (002) peak position shows that film is suffered from strain. All of the peaks can be indexed to cubic BTO (JCPDS 89-2475). This XRD patterns observed no splitting of peak (200) at 2θ =44.3°, as shown by inset figure, which specify the cubic structure of the fabricated BTO thin film. This may be caused by the presence of a small spontaneous lattice strain. X. Yang et. al. and A.A. Thanki and his colleague also observed the XRD diffraction peak without splitting [36, 37]. The Scherrer formula was used to determine the size of crystallite 'D' [38].

$$D = \frac{k}{w \cos \theta} \dots\dots\dots (10)$$

Where k represents Scherrer constant (0.94), λ is the wavelength of the x-rays used (Cu Kα average = 1.54178 Å), w is the FWHM of (200) diffraction peak and θ is the Bragg's diffraction angle. After calculation, the crystallite size of BTO thin film has been observed to be 32.021 nm. Dislocation density 'ρ' which represents the amount of defect, was evaluated using relation given below [39]

$$\rho = \frac{1}{D^2} \dots\dots\dots (2)$$

The calculated value of dislocation density is 8.04484 x 10<sup>-4</sup> nm<sup>-2</sup>.

## 2.2. SEM Analysis

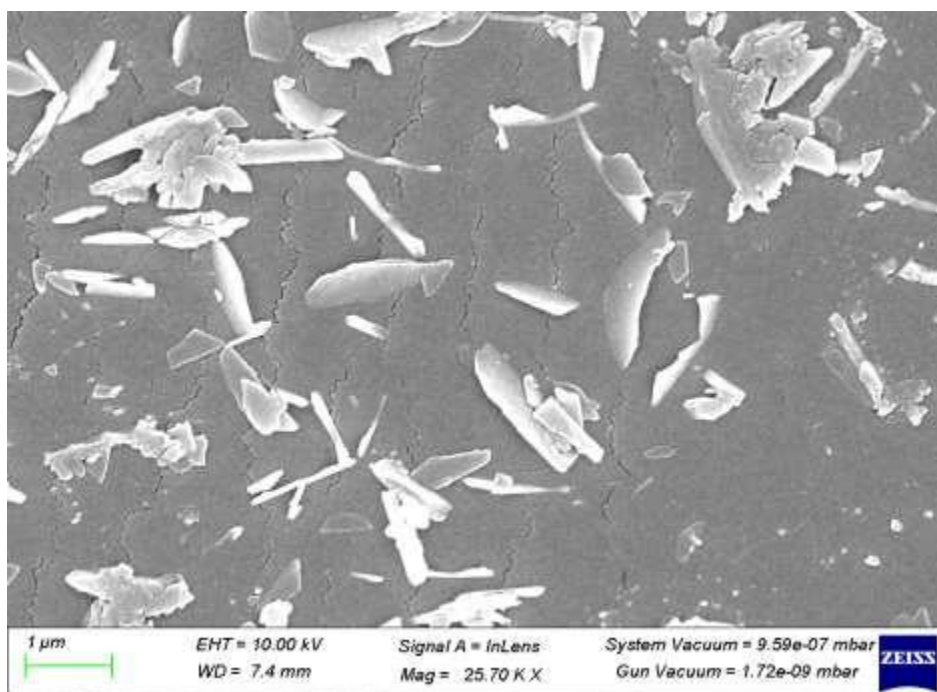


Fig. 3: SEM micrograph of BTO thin film.

Figure 3, represents the SEM micrograph of BTO thin film fabricated on the quartz substrate using sol gel technique. SEM analysis observed the dense thin films with cracks on its surface. Flat flakes with irregular shapes have also been observed on the surface of the film.

### EDX Analysis

The composition of the BTO thin film produced by the sol gel deposition process on quartz substrate was determined by energy dispersive X-ray analysis (EDX). BTO had no contaminants, according to the results of the EDX investigation. The EDX spectrum of the BTO thin film is shown in fig. 4. The EDX patterns made obvious that the Ba and Ti element's high intensity peaks were present. The comparison of Ba, Ti, and O composition percentages in the thin film is shown in the inset table. The created BTO thin film is incredibly pure, as demonstrated by this result.



Figure 4. EDX analysis of BTO thin film, inset table shows the percentage composition of Ba, Ti and O

### 2.3. UV-Vis Spectroscopy

Figure 5 shows the transmittance and absorption spectra of BTO thin film. It is clear from the figure that transmittance increase in 400-700 nm range and film is highly transparent above 530 nm with transmittance >90%. The transmittance of the thin film falls sharply for the wavelength < 465 nm, revealing inter-band transitions [40,41]. The inset diagram shows high absorbance in short wavelength region (~215nm). The absorption edge was observed at 299 nm. The curves in the transmittance graph show a well-defined interference fringe pattern, thus indicating the smooth surface and relatively good homogeneity of the film, which is in agreement with literature [42, 43]. Transmission is extremely high in longer wavelength region because the higher wavelengths cannot support the necessary electronic transitions [44]

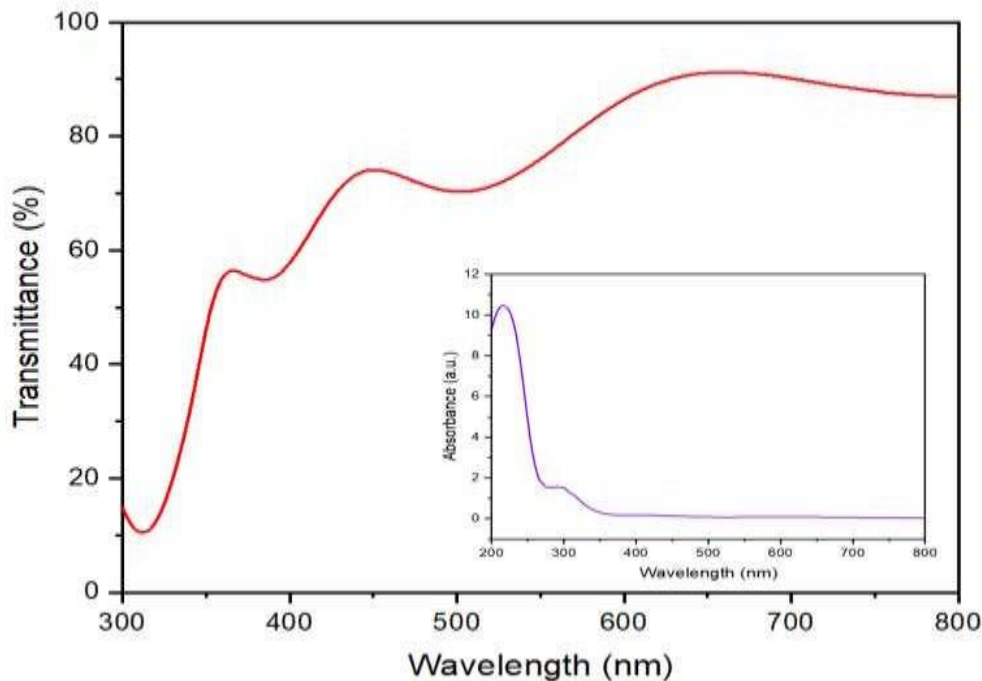


Fig. 5. UV spectrum for BTO thin film.

The optical band gap energy ( $E_g$ ) was estimated by the Tauc plot (shown by figure 6 (a)). The band gap was obtained by extrapolating the linear portion of the curve  $(\alpha h\nu)^2$  to zero value of  $h\nu$  and the observed value of  $E_g$  is 3.77 eV [45]. As the Urbach energy ( $E_u$ ) is interrelated to the number of defects in the film [46]. Its value can be estimated by plotting a graph between  $\ln(\alpha)$  and  $h\nu$  and then finding out the slope as shown by fig. 6(b). One can find out the value  $E_u$  by taking reciprocal of the slope and in this report the value of  $E_u$  is estimated to be 0.34456 eV.

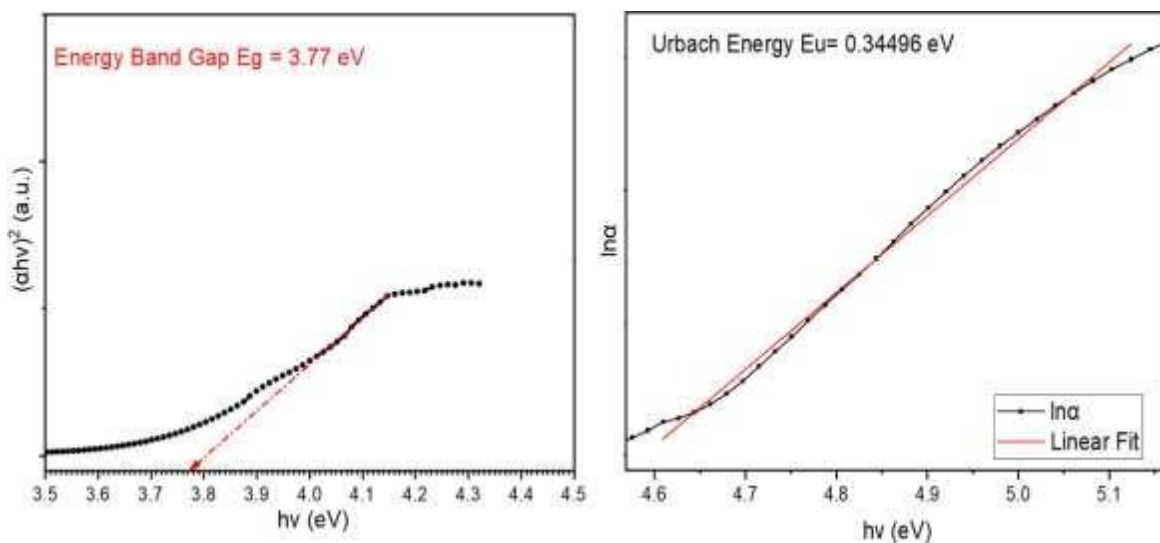


Fig. 6.(a) Plots of  $(\alpha h\nu)^2$  vs.  $h\nu$  describing band gap for BTO thin film (b) Linear fit for the determination of Urbach energy

### **3. Conclusion**

High quality BTO thin film was deposited onto the quartz substrate using technique of sol gel . X-ray diffraction patterns revealed the cubic structure of the BTO thin film. The calculated values of crystallite size and dislocation density are 32.021 nm and  $8.04484 \times 10^{-4} \text{ nm}^{-2}$  respectively. SEM images displayed uniform dense thin film with presence of cracks and flakes on the surface. EDX study confirmed the presence of barium, titanium and oxygen. High transmittance was observed for the thin film in visible region. The optical band gap and Urbach energy were estimated to value 3.7 eV and 0.34456 eV respectively. The wide and direct band gap of BTO film is applicable for many optoelectronic devices.

### **Acknowledgements**

The authors wish to acknowledge Dr. Arjun Singh, ITM University, Gurugram, India for their help in characterization part for this research work.

### **References**

- [1] R. Ashiri, A. Nemati, M. Sasani Ghamsari, and H. Aadelkhani, "Characterization of optical properties of amorphous BaTiO<sub>3</sub> nanothin films," *J. Non. Cryst. Solids*, vol. 355, no. 50–51, pp. 2480–2484, 2009, doi: 10.1016/j.jnoncrysol.2009.08.030.
- [2] B. Bihari, J. Kumar, G. T. Stauff, P. C. Van Buskirk, and S. H. Cheol, "Investigation of barium titanate thin films on MgO substrates by second-harmonic generation," *J. Appl. Phys.*, vol. 76, no. 2, pp. 1169–1174, 1994, doi: 10.1063/1.357841.
- [3] T. Horikawa et al., "Dielectric properties of (Ba, Sr)TiO<sub>3</sub> thin films deposited by Rf sputtering," *Jpn. J. Appl. Phys.*, vol. 32, no. 9, pp. 4126–4130, 1993, doi: 10.1143/JJAP.32.4126.
- [4] [1] D. M. Gill, B. A. Block, C. W. Conrad, B. W. Wessels, and S. T. Ho, "Thin film channel waveguides fabricated in metalorganic chemical vapor deposition grown BaTiO<sub>3</sub> on MgO," *Appl. Phys. Lett.*, vol. 69, no. 20, pp. 2968–2970, 1996, doi: 10.1063/1.117746.
- [5] A. Karvounis, F. Timpu, V. V. Vogler-Neuling, R. Savo, and R. Grange, "Barium Titanate Nanostructures and Thin Films for Photonics," *Advanced Optical Materials*, vol. 8, no. 24. 2020, doi: 10.1002/adom.202001249.
- [6] J. Yuk and T. Troczynski, "Sol-gel BaTiO<sub>3</sub> thin film for humidity sensors," *Sensors Actuators, B Chem.*, vol. 94, no. 3, pp. 290–293, 2003, doi: 10.1016/S0925-4005(03)00371-X.
- [7] M. Singh, B. C. Yadav, A. Ranjan, M. Kaur, and S. K. Gupta, "Synthesis and characterization of perovskite barium titanate thin film and its application as LPG sensor," *Sensors Actuators, B Chem.*, vol. 241, no. March 2019, pp. 1170–1178, 2017, doi: 10.1016/j.snb.2016.10.018.
- [8] F. He, W. Ren, G. Liang, P. Shi, X. Wu, and X. Chen, "Structure and dielectric properties of barium titanate thin films for capacitor applications," *Ceram. Int.*, vol. 39, no. SUPPL.1, pp. 1–5, 2013, doi: 10.1016/j.ceramint.2012.10.118.
- [9] G. J. Reynolds, M. Kratzer, M. Dubs, H. Felzer, and R. Mamazza, "Sputtered Modified Barium Titanate for Thin-Film Capacitor Applications," *Materials (Basel)*, vol. 5, no. 12, pp. 575–589, 2012, doi: 10.3390/ma5040575.

- [10] L. Stoica, F. Bygrave, and A. J. Bell, "Barium titanate thin films for novel memory applications," *UPB Sci. Bull. Ser. A Appl. Math. Phys.*, vol. 75, no. 3, pp. 147–158, 2013.
- [11] K. H. Chen, Y. C. Chen, Z. S. Chen, C. F. Yang, and T. C. Chang, "Temperature and frequency dependence of the ferroelectric characteristics of BaTiO<sub>3</sub> thin films for nonvolatile memory applications," *Appl. Phys. A Mater. Sci. Process.*, vol. 89, no. 2, pp. 533–536, 2007, doi: 10.1007/s00339-007-4108-4.
- [12] N. Golego, S. A. Studenikin, and M. Cocivera, "Properties of Dielectric BaTiO<sub>3</sub> Thin Films Prepared by Spray Pyrolysis," *Chem. Mater.*, vol. 10, no. 7, pp. 2000–2005, 1998, doi: 10.1021/cm980153+.
- [13] V. M. Fuenzalida, J. G. Lisoni, N. I. Morimoto, and J. C. Acquadro, "Tetragonal BaTiO<sub>3</sub> thin films hydrothermally grown on TiO<sub>2</sub> single crystals," *Appl. Surf. Sci.*, vol. 108, no. 3, pp. 385–389, 1997, doi: 10.1016/S0169-4332(96)00610-1.
- [14] V. P. Dravid, H. Zhang, L. A. Wills, and B. W. Wessels, "On the Microstructure, Chemistry, and Dielectric Function of BaTiO<sub>3</sub>MOCVD Thin Films," *J. Mater. Res.*, vol. 9, no. 2, pp. 426–430, 1994, doi: 10.1557/JMR.1994.0426.
- [15] D. L. Kaiser *et al.*, "Epitaxial growth of BaTiO<sub>3</sub> thin films at 600°C by metalorganic chemical vapor deposition," *Appl. Phys. Lett.*, vol. 2801, no. 1995, p. 2801, 1995, doi: 10.1063/1.113480.
- [16] M. Si, "Preparation and characterization of BaTiO<sub>3</sub> thin films on," vol. 12, no. 4, pp. 34–38, 1997.
- [17] N. Wang *et al.*, "Morphology and microstructure of BaTiO<sub>3</sub>/SrTiO<sub>3</sub> superlattices grown on SrTiO<sub>3</sub> by laser molecular-beam epitaxy," *Appl. Phys. Lett.*, vol. 75, no. 22, pp. 3464–3466, 1999, doi: 10.1063/1.125297.
- [18] S. Kim, S. Hishita, Y. M. Kang, and S. Baik, "Structural characterization of epitaxial BaTiO<sub>3</sub> thin films grown by sputter deposition on MgO(100)," *J. Appl. Phys.*, vol. 78, no. 9, pp. 5604–5608, 1995, doi: 10.1063/1.360696.
- [19] M. N. Kamalasanan, N. D. Kumar, and S. Chandra, "Structural and microstructural evolution of barium titanate thin films deposited by the sol-gel process," *J. Appl. Phys.*, vol. 76, no. 8, pp. 4603–4609, 1994, doi: 10.1063/1.358493.
- [20] M. Cernea, "Methods for preparation of BaTiO<sub>3</sub> thin films," *J. Optoelectron. Adv. Mater.*, vol. 6, no. 4, pp. 1349–1356, 2004.
- [21] S. S. Kumbhar *et al.*, "Structural and electrical properties of barium titanate (BaTiO<sub>3</sub>) thin films obtained by spray pyrolysis method," *Mater. Sci. Pol.*, vol. 2015, no. 4, pp. 852–861, 2015, doi: 10.1515/msp-2015-0107.
- [22] S. P. More and R. J. Topare, "The review of various synthesis methods of barium titanate with the enhanced dielectric properties," *AIP Conf. Proc.*, vol. 1728, no. 2016, pp. 1–7, 2016, doi: 10.1063/1.4946611.
- [23] H. Kumazawa and K. Masuda, "Fabrication of barium titanate thin films with a high dielectric constant by a sol-gel technique," *Thin Solid Films*, vol. 353, no. 1, pp. 144–148, 1999, doi: 10.1016/S0040-6090(99)00427-7.



- [24] S. Kim and O. Y. Kwon, "Barium titanate thin films prepared on MgO (100) substrates by coating-pyrolysis process," *Korean J. Chem. Eng.*, vol. 16, no. 1, pp. 40–44, 1999, doi: 10.1007/BF02699003.
- [25] T. Hayashi, N. Ohji, K. Hirohara, T. Fukunaga, and H. Maiwa, "Preparation and properties of ferroelectric batio<sub>3</sub> thin films by sol-gel process," *Jpn. J. Appl. Phys.*, vol. 32, no. 9, pp. 4092–4094, 1993, doi: 10.1143/JJAP.32.4092.
- [26] R. Thomas, D. C. Dube, M. N. Kamalasanan, and S. Chandra, "Optical and electrical properties of BaTiO<sub>3</sub> thin films prepared by chemical solution deposition," *Thin Solid Films*, vol. 346, no. 1, pp. 212–225, 1999, doi: 10.1016/S0040-6090(98)01772-6.
- [27] W. Ousi-Benommar, S. S. Xue, R. A. Lessard, A. Singh, Z. L. Wu, and P. K. Kuo, "Structural and optical characterization of BaTiO<sub>3</sub> thin films prepared by metal-organic deposition from barium 2-ethylhexanoate and titanium dimethoxy dineodecanoate," *J. Mater. Res.*, vol. 9, no. 4, pp. 970–979, 1994, doi: 10.1557/JMR.1994.0970.
- [28] H. Basantakumar Sharma and H. N. K. Sarma, "Electrical properties of sol-gel processed barium titanate films," *Thin Solid Films*, vol. 330, no. 2, pp. 178–182, 1998, doi: 10.1016/S0040-6090(98)00551-3.
- [29] R. Ashiri, A. Nemati, and M. Sasani Ghamsari, "Crack-free nanostructured BaTiO<sub>3</sub> thin films prepared by sol-gel dip-coating technique," *Ceram. Int.*, vol. 40, no. 6, pp. 8613–8619, 2014, doi: 10.1016/j.ceramint.2014.01.078.
- [30] K. Bakken, A. B. Blichfeld, D. Chernyshov, T. Grande, J. Glaum, and M. A. Einarsrud, "Mechanisms for texture in BaTiO<sub>3</sub> thin films from aqueous chemical solution deposition," *J. Sol-Gel Sci. Technol.*, vol. 95, no. 3, pp. 562–572, 2020, doi: 10.1007/s10971-020-05356-2.
- [31] J. Vukmirović, D. Tripković, B. Bajac, S. Kojić, G. M. Stojanović, and V. V. Srdić, "Comparison of barium titanate thin films prepared by inkjet printing and spin coating," *Process. Appl. Ceram.*, vol. 9, no. 3, pp. 151–156, 2015, doi: 10.2298/PAC1503151V.
- [32] H. X. Zhang *et al.*, "Optical and electrical properties of sol-gel derived BaTiO<sub>3</sub> films on ITO coated glass," *Mater. Chem. Phys.*, vol. 63, no. 2, pp. 174–177, 2000, doi: 10.1016/S0254-0584(99)00222-9.
- [33] T. Hayashi, N. Ohji, K. Hirohara, T. Fukunaga, and H. Maiwa, "Preparation and properties of ferroelectric batio<sub>3</sub> thin films by sol-gel process," *Jpn. J. Appl. Phys.*, vol. 32, no. 9, pp. 4092–4094, 1993, doi: 10.1143/JJAP.32.4092.
- [34] L. L. Hench and J. K. West, "The Sol-Gel Process," *Chem. Rev.*, vol. 90, no. 1, pp. 33–72, 1990, doi: 10.1021/cr00099a003.
- [35] C. J. Brinker, G. C. Frye, A. J. Hurd, and C. S. Ashley, "Fundamentals of sol-gel dip coating,"
- [36] A. A. Thanki and R. K. Goyal, "Study on effect of cubic- and tetragonal phased BaTiO<sub>3</sub> on the electrical and thermal properties of polymeric nanocomposites," *Mater. Chem. Phys.*, vol. 183, pp. 447–456, 2016, doi: 10.1016/j.matchemphys.2016.08.052.

- [37] X. Yang et al., “Colossal dielectric performance of pure barium titanate ceramics consolidated by spark plasma sintering,” *RSC Adv.*, vol. 6, no. 79, pp. 75422–75429, 2016, doi: 10.1039/c6ra14741k.
- [38] Y. Ma, Y. C. Chang, and J. Z. Yin, “Evaluation of lattice strain in ZnO thin films based on Williamson-Hall analysis,” *J. Optoelectron. Adv. Mater.*, vol. 21, no. 11–12, pp. 702–709, 2019.
- [39] A. Chelouche, D. Djouadi, H. Merzouk, and A. Aksas, “Influence of Ag doping on structural and optical properties of ZnO thin films synthesized by the sol-gel technique,” *Appl. Phys. A Mater. Sci. Process.*, vol. 115, no. 2, pp. 613–616, 2014, doi: 10.1007/s00339-013-8029-0.
- [40] R. Ashiri, A. Nemati, M. Sasani Ghamsari, and H. Aadelkhani, “Characterization of optical properties of amorphous BaTiO<sub>3</sub> nanothin films,” *J. Non. Cryst. Solids*, vol. 355, no. 50–51, pp. 2480–2484, 2009, doi: 10.1016/j.jnoncrsol.2009.08.030.
- [41] H. X. Zhang et al., “Optical and electrical properties of sol-gel derived BaTiO<sub>3</sub> films on ITO coated glass,” *Mater. Chem. Phys.*, vol. 63, no. 2, pp. 174–177, 2000, doi: 10.1016/S0254-0584(99)00222-9.
- [42] G. Kaur, A. Mitra, and K. L. Yadav, “Pulsed laser deposited Al-doped ZnO thin films for optical applications,” *Prog. Nat. Sci. Mater. Int.*, vol. 25, no. 1, pp. 12–21, 2015, doi: 10.1016/j.pnsc.2015.01.012.
- [43] F. M. Pontes et al., “Ferroelectric and optical properties of Ba<sub>0.8</sub>Sr<sub>0.2</sub>TiO<sub>3</sub> thin film,” *J. Appl. Phys.*, vol. 91, no. 9, pp. 5972–5978, 2002, doi: 10.1063/1.1466526.
- [44] N. M. Ahmed, Z. Sauli, U. Hashim, and Y. Al-douri, “Investigation of the absorption coefficient, refractive index, energy band gap, and film thickness for Al<sub>0.11</sub>Ga<sub>0.89</sub>N by optical transmission method,” *Int. J. Nanoelectron. Mater.*, vol. 2, no. December 2015, pp. 189–195, 2009.
- [45] S. Acharya, “Ultrafast charge carrier dynamics of ZnO thin films and BaTiO<sub>3</sub>-ZnO heterostructures,” 2013.
- [46] D. T. Speaks, “Effect of concentration, aging, and annealing on sol gel ZnO and Al-doped ZnO thin films,” *International Journal of Mechanical and Materials Engineering*, vol. 15, no. 1, Jan. 2020, doi: 10.1186/s40712-019-0113-6.